
Effective Data Augmentation With Diffusion Models

Anonymous Author(s)

Affiliation

Address

email

Abstract

1 Data augmentation is one of the most prevalent tools in deep learning, underpinning
2 many recent advances, including those from classification, generative models, and
3 representation learning. The standard approach to data augmentation combines
4 simple transformations like rotations and flips to generate new images from existing
5 ones. However, these new images lack diversity along key semantic axes present in
6 the data. Current augmentations cannot alter the high-level semantic attributes, such
7 as animal species present in a scene, to enhance the diversity of data. We address
8 the lack of diversity in data augmentation with image-to-image transformations
9 parameterized by pre-trained text-to-image diffusion models. Our method edits
10 images to change their semantics using an off-the-shelf diffusion model, and
11 generalizes to novel visual concepts from a few labelled examples. We evaluate
12 our approach on few-shot image classification tasks, and on a real-world weed
13 recognition task, and observe an improvement in accuracy in tested domains.

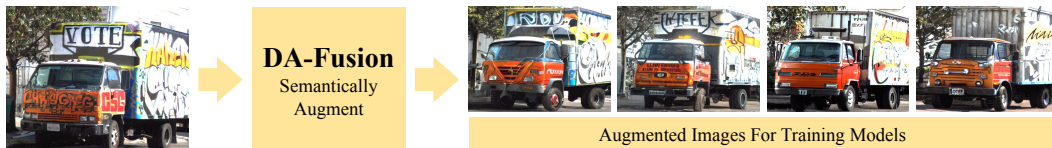


Figure 1: Real images (left) are semantically modified using a publicly available off-the-shelf Stable Diffusion checkpoint. Resulting synthetic images (right) are used for training downstream classification models.

14 1 Introduction

15 An omnipresent lesson in deep learning is the importance of internet-scale data, such as ImageNet
16 [Deng et al., 2009], JFT [Sun et al., 2017], OpenImages [Kuznetsova et al., 2018], and LAION-5B
17 [Schuhmann et al., 2022], which are driving advances in Foundation Models [Bommasani et al.,
18 2021] for image generation. These models use large deep neural networks [Rombach et al., 2022] to
19 synthesize photo-realistic images for a rich landscape of prompts. The advent of photo-realism in
20 large generative models is driving interest in using synthetic images to augment visual recognition
21 datasets [Azizi et al., 2023]. These generative models promise to unlock diverse and large-scale
22 image datasets from just a handful of real images without the usual labelling cost.

23 Standard data augmentations aim to diversify images by composing randomly parameterized image
24 transformations [Antoniou et al., 2017, Perez and Wang, 2017, Shorten and Khoshgoftaar, 2019,
25 Zhao et al., 2020]. Transformations including flips and rotations are chosen that respect basic
26 invariances present in the data, such as horizontal reflection symmetry for a coffee mug. Basic image
27 transformations are thoroughly explored in the existing data augmentation literature, and produce
28 models that are robust to color and geometry transformations. However, models for recognizing
29 coffee mugs should also be sensitive to subtle details of visual appearance like the brand of mug; yet,
30 basic transformations do not produce novel structural elements, textures, or changes in perspective.
31 On the other hand, large pretrained generative models have become exceptionally sensitive to subtle
32 visual details, able to generate uniquely designed mugs from a single example [Gal et al., 2022].

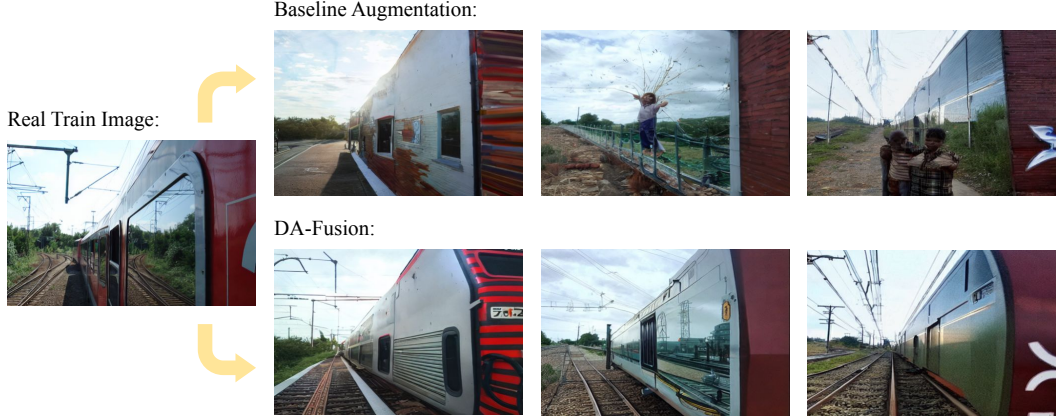


Figure 2: DA-Fusion produces task-relevant augmentations with no prior knowledge about the image content. Given an image of a train from PASCAL VOC [Everingham et al., 2009], we generate several augmentations using Real Guidance [He et al., 2022] (top row), and compare these to our method (bottom row).

33 Our key insight is that large pretrained generative models *complement the weaknesses* of standard
 34 data augmentations, while *retaining the strengths*: universality, controllability, and performance. We
 35 propose a flexible data augmentation strategy that generates variations of real images using text-to-
 36 image diffusion models (DA-Fusion). Our method adapts the diffusion model to new domains by
 37 fine-tuning pseudo-prompts in the text encoder representing concepts to augment. DA-Fusion modifies
 38 the appearance of objects in a manner that respects their semantic invariances, such as the design of the
 39 graffiti on the truck in Figure 1 and the design of the train in Figure 2. We test our method on few-shot
 40 image classification tasks with common and rare concepts, including a real-world weed recognition
 41 task the diffusion model has not seen before. Using the same hyper-parameters in all domains,
 42 our method outperforms prior work, improving data augmentation by up to +10 percentage points.
 43 Our ablations illustrate that DA-Fusion produces **larger gains for the more fine-grain concepts**.
 44 Open-source code is released at: <https://github.com/anonymous-da-fusion/da-fusion>.

45 2 Data Augmentation With Diffusion Models

46 In this work we develop a flexible data augmentation strategy using text-to-image diffusion models.
 47 In doing so, we consider *three desiderata*: Our method is 1) **universal**: it produces high-fidelity
 48 augmentations for new and fine-grain concepts, not just the ones the diffusion model was trained on;
 49 2) **controllable**: the content, extent, and randomness of the augmentation are simple to control and
 50 straightforward to tune; 3) **performant**: gains in accuracy justify the additional computational cost
 51 of generating images from Stable Diffusion. We discuss these in the following sections.

52 2.1 A Universal Generative Data Augmentation

53 Standard data augmentations apply to all images regardless of class and content Perez and Wang
 54 [2017]. We aim to capture this flexibility with our diffusion-based augmentation. This is challenging
 55 because real images may contain elements the diffusion model is not able to generate out-of-the-box.
 56 How do we generate plausible augmentations for such images? Shown in Figure 3, we adapt the
 57 diffusion model to new concepts by inserting c new embeddings in the text encoder of the generative
 58 model, and fine-tuning only these embeddings to maximize the likelihood of generating new concepts.

59 **Adapting Generative Model** When generating synthetic images, previous work uses a prompt with
 60 the specified class name He et al. [2022]. However, this is not possible for concepts that lie outside
 61 the vocabulary of the generative model because the model’s text encoder has not learned words to
 62 describe these concepts. We discuss this problem in Section A with our contributed weed-recognition
 63 task, which our pretrained diffusion model is unable to generate when the class name is provided. A
 64 simple solution to this problem is to have the model’s text encoder learn new words to describe new
 65 concepts. Textual Inversion [Gal et al., 2022] is well-suited for this, and we use it to learn a word
 66 embedding \vec{w}_i from a handful of labelled images for each class in the dataset.

$$\min_{\vec{w}_0, \vec{w}_1, \dots, \vec{w}_c} \mathbb{E} \left[\|\epsilon - \epsilon_\theta(\sqrt{\tilde{\alpha}_t}x_0 + \sqrt{1 - \tilde{\alpha}_t}\epsilon, t, \text{"a photo of a } \vec{w}_i\text{"})\|^2 \right] \quad (1)$$

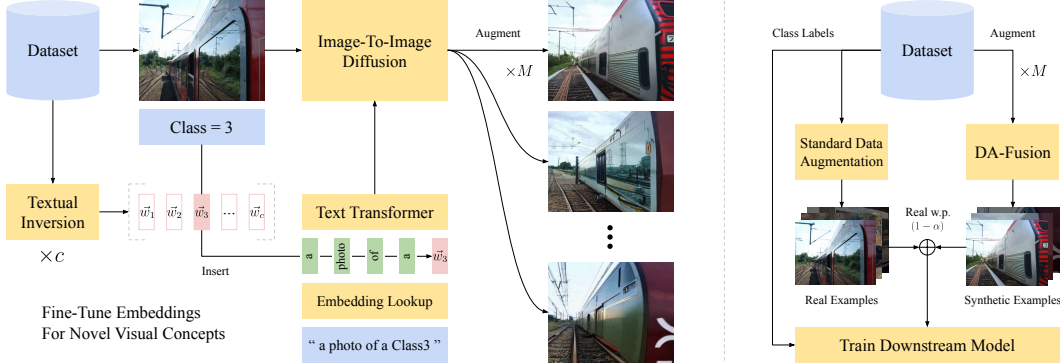


Figure 3: How our data augmentation works. Given a dataset of images and their class labels, we generate M augmented versions of each real image using an image-editing technique and a pretrained Stable Diffusion checkpoint. Synthetic images are mixed with real data when training downstream models.

67 We initialize each new embedding \bar{w}_i to a class-agnostic value (see Appendix K), and optimize them
 68 to minimize the simplified loss function proposed by Ho et al. [2020]. Figure 3 shows how new
 69 embeddings \bar{w}_i are inserted in the prompt given an image of a train. Our method is modular, and as
 70 other mechanisms are studied for adapting diffusion models, Textual Inversion can easily be swapped
 71 out with one of these, and the quality of the augmentations from DA-Fusion can be improved.

72 **Generating Synthetic Images** Many of the existing approaches generate synthetic images from
 73 scratch Antoniou et al. [2017], Tanaka and Aranha [2019], Besnier et al. [2020], Zhang et al. [2021b,a].
 74 This is particularly challenging for concepts the diffusion model hasn’t seen before. Rather than
 75 generate from scratch, we use real images as a guide. We splice real images into the generation
 76 process of the diffusion model following prior work in SDEdit Meng et al. [2022]. Given a reverse
 77 diffusion process with S steps, we insert a real image x_0^{ref} with noise $\epsilon \sim \mathcal{N}(0, I)$ at timestep $\lfloor St_0 \rfloor$,
 78 where $t_0 \in [0, 1]$ is a hyperparameter controlling the insertion position of the image.

$$x_{\lfloor St_0 \rfloor} = \sqrt{\tilde{\alpha}_{\lfloor St_0 \rfloor}} x_0^{\text{ref}} + \sqrt{1 - \tilde{\alpha}_{\lfloor St_0 \rfloor}} \epsilon \quad (2)$$

79 We proceed with reverse diffusion starting from the spliced image at timestep $\lfloor St_0 \rfloor$ and iterating
 80 Equation 5 until a sample is generated at timestep 0. Generation is guided with a prompt that includes
 81 the new embedding \bar{w}_i for the class of the source image (see Appendix K for prompt details).

82 2.2 Controlling Augmentation

83 **Improving Diversity By Randomizing Intensity** Having appropriately balanced real and synthetic
 84 images, our goal is to maximize diversity. This goal is shared with standard data augmentation Perez
 85 and Wang [2017], Shorten and Khoshgoftaar [2019], where multiple simple transformations are
 86 used, yielding more diverse data. Despite the importance of diversity, generative models typically
 87 employ frozen sampling hyperparameters to produce synthetic datasets Antoniou et al. [2017],
 88 Tanaka and Aranha [2019], Yamaguchi et al. [2020], Zhang et al. [2021b,a], He et al. [2022]. Inspired
 89 randomization in standard data augmentations (such as the angle of rotation), we randomly sample
 90 the insertion position t_0 where real images are spliced into Equation 2. This randomizes the extent
 91 images are modified—as $t_0 \rightarrow 0$ generations more closely resemble the guide image.

92 In Section 3.2 we sample uniformly at random $t_0 \sim \mathcal{U}(\{\frac{1}{k}, \frac{2}{k}, \dots, \frac{k}{k}\})$, and observe a consistent
 93 improvement in classification accuracy with $k = 4$ compared to fixing t_0 . Though the hyperparameter
 94 t_0 is perhaps the most direct translation of randomized intensity to generative model-based data
 95 augmentations, there are several alternatives. For example, one may consider the guidance scale
 96 parameter used in classifier-free guidance [Ho and Salimans, 2022]. We leave this as future work.

97 3 DA-Fusion Improves Few-Shot Classification

98 **Experimental Details** We test few-shot classification on seven datasets with three data augmenta-
 99 tion strategies. RandAugment [Cubuk et al., 2020] employs no synthetic images, and uses the default

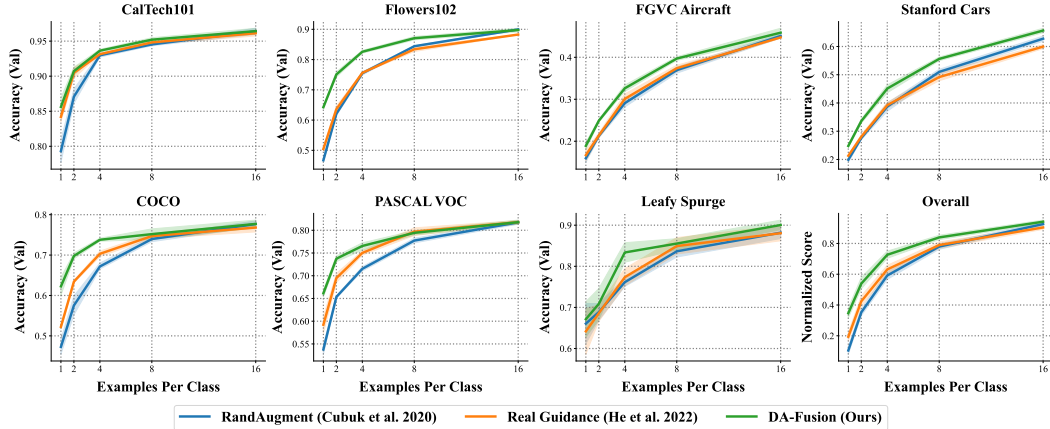


Figure 4: Few-shot classification performance with full information. DA-Fusion consistently outperforms RandAugment [Cubuk et al., 2020], and Real Guidance [He et al., 2022] with a descriptive prompt. In fine-grain domains such as Flowers102, which represents classification of flowers into subclasses like "giant white arum lily," Real Guidance performs no better than traditional data augmentation. In contrast, DA-Fusion performs consistently well across a variety of domains with common concepts (COCO, PASCAL VOC, Caltech101), rare concepts (Flowers102, FGVC Aircraft, Stanford Cars) and novel concepts to Stable Diffusion (Leafy Spurge).

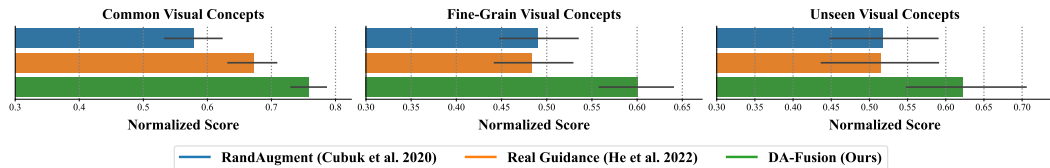


Figure 5: Performance stratified by concept novelty. Real Guidance [He et al., 2022] uses a descriptive prompt to instruct Stable Diffusion what to augment, and works for common concepts Stable Diffusion was trained on. However, for harder-to-describe concepts, this strategy fails. DA-Fusion works well at all novelty levels, improving by 12.8% for common concepts, 24.2% for fine-grain concepts, and 20.8% for unseen concepts.

100 hyperparameters in `torchvision`. Real Guidance [He et al., 2022] uses SDEdit on real images with
 101 $t_0 = 0.5$, has a descriptive prompt about the class, and shares hyperparameters with our method to
 102 ensure fair evaluation. DA-Fusion is prompted with "a photo of a $\langle w_i \rangle$ " where the embedding for
 103 $\langle w_i \rangle$ is initialized to the embedding of the class name and learned according to Section 2.1.

104 Each real image is augmented M times, and a ResNet50 classifier pre-trained on ImageNet is fine-
 105 tuned on a mixture of real and synthetic images sampled as discussed in Section 2.2. We vary the
 106 number of examples per class used for training the classifier on the x-axis in the following plots,
 107 and fine-tune the final linear layer of the classifier for 10,000 steps with a batch size of 32 and the
 108 Adam optimizer with learning rate 0.0001. We record validation metrics every 200 steps and report
 109 the epoch with highest accuracy. Solid lines in plots represent means, and error bars denote 68%
 110 confidence intervals over 4 independent trials. An overall score is calculated for all datasets after
 111 normalizing performance using $y_i^{(d)} \leftarrow (y_i^{(d)} - y_{\min}^{(d)}) / (y_{\max}^{(d)} - y_{\min}^{(d)})$, where d represents the dataset,
 112 $y_{\max}^{(d)}$ is the maximum performance for any trial of any method, and $y_{\min}^{(d)}$ is defined similarly.

113 **Interpreting Results** Results in Figure 4 show DA-Fusion improves accuracy in every domain,
 114 often by a significant margin when there are few real images per class. We observe gains between +5
 115 and +15 accuracy points in all seven domains compared to standard data augmentation. Our results
 116 show how generative data augmentation can significantly outperform color and geometry-based
 117 transformations like those in RandAugment [Cubuk et al., 2020]. Despite using a powerful generative
 118 model with a descriptive prompt, Real Guidance He et al. [2022] performs inconsistently, and in
 119 several domains fails to beat RandAugment. To understand this behavior, we binned the results
 120 by whether a dataset contains common concepts (COCO, PASCAL VOC, Caltech101), fine-grain
 121 concepts (Flowers102, FGVC Aircraft, Stanford Cars), or completely new concepts (Leafy Spurge),
 122 and visualized the normalized scores for the three data augmentation methods in Figure 5.

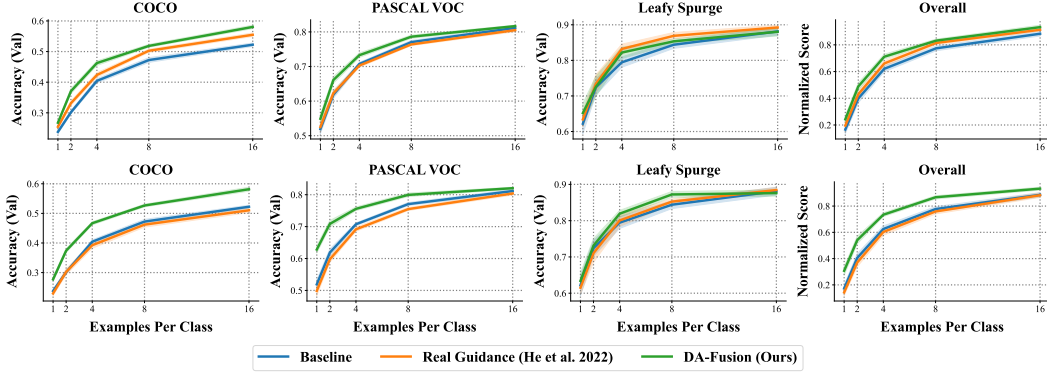


Figure 6: Few-shot classification performance with model-centric leakage prevention (top row) and data-centric leakage prevention (bottom row). DA-Fusion performs well even when evaluated on new visual concepts.

123 **Class Novelty Hinders Real Guidance** Figure 5 reveals a systematic failure mode in Real Guidance
 124 [He et al., 2022] for novel and fine-grain concepts. These concepts are harder to describe in a prompt
 125 than common ones—consider the prompts "a top-down drone image of leafy spurge taken from 100ft
 126 in the air above a grassy field" versus "a photo of a cat." DA-Fusion mitigates this by optimizing
 127 pseudo-prompts, formatted as "a photo of a $\langle w_i \rangle$ ", that instruct the diffusion model on what to
 128 generate, and has the added benefit of requiring no prompt engineering. Our method works well at all
 129 levels of concept novelty, and produces larger gains the more fine-grain concepts are, improving by
 130 12.8% for common concepts, 24.2% for fine-grain concepts, and 20.8% for novel concepts.

131 3.1 Preventing Leakage Of Internet Data

132 Previous work utilizing large pretrained generative models to produce synthetic data [He et al., 2022]
 133 has left an important question unanswered: *are we sure they are working for the right reason?*
 134 Models trained on internet data have likely seen many examples of classes in common benchmarking
 135 datasets like ImageNet Deng et al. [2009]. Moreover, Carlini et al. [2023] have recently shown that
 136 pretrained diffusion models can leak their training data. Leakage of internet data, as in Figure 8, risks
 137 compromising evaluation. Suppose our goal is to test how images from diffusion models improve
 138 few-shot classification with only a few real images, but leakage of internet data gives our classifier
 139 access to thousands of real images. Performance gains observed may not reflect the quality of the
 140 data augmentation methodology itself, and may lead to drawing the wrong conclusions.

141 We explore two methods for preventing leakage of Stable Diffusion’s training data. We first consider a
 142 *model-centric* approach that prevents leakage by editing the model weights to remove class knowledge.
 143 We also consider a *data-centric* approach that hides class information from the model inputs.

144 **Model-Centric Leakage Prevention** Our goal with this approach is to remove knowledge about
 145 concepts in our benchmarking datasets from the weights of Stable Diffusion. We accomplish this by
 146 fine-tuning Stable Diffusion in order to remove the ability to generate concepts from our benchmarking
 147 datasets. Given a list of class names in these datasets, we utilize a recent method developed by
 148 Gandikota et al. [2023] that fine-tunes the UNet backbone of Stable Diffusion so that concepts
 149 specified by a given prompt can no longer be generated (we use class names as such prompts). In
 150 particular, the UNet is fine-tuned to minimize the following loss function.

$$\min_{\theta} \mathbb{E} \left[\left\| \epsilon_{\theta}(x_t, t, \text{"class name"}) - \epsilon_{\theta^*}(x_t, t) + \eta(\epsilon_{\theta^*}(x_t, t, \text{"class name"}) - \epsilon_{\theta^*}(x_t, t)) \right\|^2 \right] \quad (3)$$

151 Where "class name" is replaced with the actual class name of the concept being erased, θ represents
 152 the parameters of the UNet being fine-tuned, and θ^* represents the initial parameters of the UNet.
 153 This procedure, named ESD by Gandikota et al. [2023], can be interpreted as guiding generation in
 154 the opposite direction of classifier free-guidance, and can erase a variety of types of concepts.

155 **Data-Centric Leakage Prevention** While editing the model directly to remove knowledge about
 156 classes is a strong defense against possible leakage, it is also costly. In our experiments, erasing a
 157 single class from Stable Diffusion takes two hours on a single 32GB V100 GPU. As an alternative
 158 for situations where the cost of a model-centric defense is too high, we can achieve a weaker defense

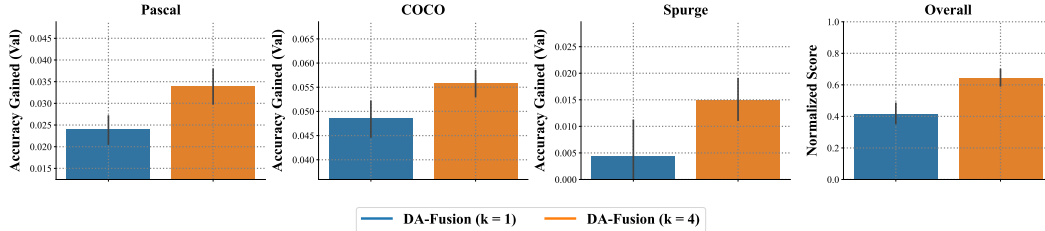


Figure 7: Ablation for randomizing augmentation intensity. We vary the number of intensities from ($k = 4$) in the main experiments, to a deterministic insertion position $t_0 = 0.5$. We report the gain in average few-shot classification accuracy over standard data augmentation, and observe a consistent improvement.

159 by removing all mentions of the class name from the inputs of the model. In practice, switching from
 160 a prompt that has the class name to a new prompt omitting the class name is sufficient.

161 **Results With Model-Centric Leakage Prevention** Figure 6 shows results when erasing class
 162 knowledge from Stable Diffusion weights. We observe a consistent improvement in validation
 163 accuracy by as much as +5 percentage points on the Pascal and COCO domains when compared
 164 to the standard data augmentation baseline. DA-Fusion exceeds performance of Real Guidance He
 165 et al. [2022] overall while utilizing the same hyperparameters, without any prior information about
 166 the classes in these datasets. In this setting, Real Guidance performs comparably to the baseline,
 167 which suggests that gains in Real Guidance may stem from information provided by the class name.
 168 This experiment shows DA-Fusion improves few-shot learning and suggests our method generalizes
 169 to concepts Stable Diffusion wasn't trained on. To understand how these gains translate to weaker
 170 defenses against training data leakage, we next evaluate our method using a data-centric strategy.

171 **Results With Data-Centric Leakage Prevention** Figure 6 shows results when class information is
 172 hidden from Stable Diffusion inputs. As before, we observe a consistent improvement in validation
 173 accuracy, by as much as +10 percentage points on the Pascal and COCO domains when compared to
 174 the standard data augmentation baseline. DA-Fusion exceeds performance of Real Guidance He et al.
 175 [2022] in all domains while utilizing the same hyperparameters, without specifying the class name as
 176 an input to the model. With a weaker defense against training data leakage, we observe larger gains
 177 with DA-Fusion. This suggests gains are due in part to accessing Stable Diffusion's prior knowledge
 178 about classes, and highlights the need for a strong leakage prevention mechanism when evaluating
 179 synthetic data from large generative models, and understanding where gains come from.

180 3.2 How Important Are Randomized Intensities?

181 Our goal in this section is to understand what fraction of gains are due to randomizing the intensity of
 182 our augmentation based on Section 2.2. We employ the same experimental settings as in Section 3,
 183 using data-centric leakage prevention, and run our method using a fixed insertion position $t_0 = 0.5$
 184 (labelled $k = 1$ in Figure 7), following the settings used with Real Guidance. In Figure 7 we
 185 report the improvement in average classification accuracy on the validation set versus standard data
 186 augmentation. These results show that both versions of our method outperform the baseline, and
 187 randomization improves our method in all domains, leading to an overall improvement of 51%.

188 4 Discussion

189 We proposed a flexible method for data augmentation based on diffusion models, DA-Fusion. Our
 190 method adapts a pretrained diffusion model to semantically modify images and produces high quality
 191 augmentations regardless of image content. Our method improves few-shot classification accuracy
 192 in tested domains, and by up to +10 percentage points on various datasets. Similarly, our method
 193 produces gains on a contributed weed-recognition dataset that lies outside the vocabulary of the
 194 diffusion model. To understand these gains, we studied how performance is impacted by potential
 195 leakage of Stable Diffusion training data. To prevent leakage during evaluation, we presented two
 196 defenses that target the model and data respectively, each on different sides of a trade-off between
 197 defense strength and computational cost. When subject to both defenses, DA-Fusion consistently
 198 improves few-shot classification accuracy, which highlights its utility for data augmentation.

References

- Giuseppe Amattulli, Sami Domisch, Mao-Ning Tuanmu, Benoit Parmentier, Ajay Ranipeta, Jeremy Malczyk, and Walter Jetz. A suite of global, cross-scale topographic variables for environmental and biodiversity modeling. *Scientific data*, 5:180040, March 2018. ISSN 2052-4463. doi: 10.1038/sdata.2018.40. URL <https://europepmc.org/articles/PMC5859920>.
- Antreas Antoniou, Amos Storkey, and Harrison Edwards. Data augmentation generative adversarial networks, 2017. URL <https://arxiv.org/abs/1711.04340>.
- Shekoofeh Azizi, Simon Kornblith, Chitwan Saharia, Mohammad Norouzi, and David J. Fleet. Synthetic data from diffusion models improves imagenet classification. *CoRR*, abs/2304.08466, 2023. doi: 10.48550/arXiv.2304.08466. URL <https://doi.org/10.48550/arXiv.2304.08466>.
- Romain Beaumont. Clip retrieval. <https://github.com/rom1504/clip-retrieval>, 2022.
- Victor Besnier, Himalaya Jain, Andrei Bursuc, Matthieu Cord, and Patrick Pérez. This dataset does not exist: Training models from generated images. In *2020 IEEE International Conference on Acoustics, Speech and Signal Processing, ICASSP 2020, Barcelona, Spain, May 4-8, 2020*, pages 1–5. IEEE, 2020. doi: 10.1109/ICASSP40776.2020.9053146. URL <https://doi.org/10.1109/ICASSP40776.2020.9053146>.
- Rishi Bommasani, Drew A. Hudson, Ehsan Adeli, Russ Altman, Simran Arora, Sydney von Arx, Michael S. Bernstein, Jeannette Bohg, Antoine Bosselut, Emma Brunskill, Erik Brynjolfsson, Shyamal Buch, Dallas Card, Rodrigo Castellon, Niladri S. Chatterji, Annie S. Chen, Kathleen Creel, Jared Quincy Davis, Dorottya Demszky, Chris Donahue, Moussa Doumbouya, Esin Durmus, Stefano Ermon, John Etchemendy, Kawin Ethayarajh, Li Fei-Fei, Chelsea Finn, Trevor Gale, Lauren Gillespie, Karan Goel, Noah D. Goodman, Shelby Grossman, Neel Guha, Tatsunori Hashimoto, Peter Henderson, John Hewitt, Daniel E. Ho, Jenny Hong, Kyle Hsu, Jing Huang, Thomas Icard, Saahil Jain, Dan Jurafsky, Pratyusha Kalluri, Siddharth Karamcheti, Geoff Keeling, Fereshthe Khani, Omar Khattab, Pang Wei Koh, Mark S. Krass, Ranjay Krishna, Rohith Kuditipudi, and et al. On the opportunities and risks of foundation models. *CoRR*, abs/2108.07258, 2021. URL <https://arxiv.org/abs/2108.07258>.
- Andrew Brock, Jeff Donahue, and Karen Simonyan. Large scale GAN training for high fidelity natural image synthesis. In *7th International Conference on Learning Representations, ICLR 2019, New Orleans, LA, USA, May 6-9, 2019*. OpenReview.net, 2019. URL <https://openreview.net/forum?id=B1xsqj09Fm>.
- Nicholas Carlini, Jamie Hayes, Milad Nasr, Matthew Jagielski, Vikash Sehwal, Florian Tramèr, Borja Balle, Daphne Ippolito, and Eric Wallace. Extracting training data from diffusion models. *CoRR*, abs/2301.13188, 2023. doi: 10.48550/arXiv.2301.13188. URL <https://doi.org/10.48550/arXiv.2301.13188>.
- Ekin Dogus Cubuk, Barret Zoph, Jonathon Shlens, and Quoc Le. Randaugment: Practical automated data augmentation with a reduced search space. In Hugo Larochelle, Marc’Aurelio Ranzato, Raia Hadsell, Maria-Florina Balcan, and Hsuan-Tien Lin, editors, *Advances in Neural Information Processing Systems 33: Annual Conference on Neural Information Processing Systems 2020, NeurIPS 2020, December 6-12, 2020, virtual*, 2020. URL <https://proceedings.neurips.cc/paper/2020/hash/d85b63ef0ccb114d0a3bb7b7d808028f-Abstract.html>.
- Pham Thanh Dat, Anuvabh Dutt, Denis Pellerin, and Georges Quénot. Classifier training from a generative model. In *2019 International Conference on Content-Based Multimedia Indexing (CBMI)*, pages 1–6, 2019. doi: 10.1109/CBMI.2019.8877479.
- Jia Deng, Wei Dong, Richard Socher, Li-Jia Li, Kai Li, and Li Fei-Fei. Imagenet: A large-scale hierarchical image database. In *2009 IEEE Computer Society Conference on Computer Vision and Pattern Recognition (CVPR 2009), 20-25 June 2009, Miami, Florida, USA*, pages 248–255. IEEE Computer Society, 2009. doi: 10.1109/CVPR.2009.5206848. URL <https://doi.org/10.1109/CVPR.2009.5206848>.

- 249 Prafulla Dhariwal and Alexander Quinn Nichol. Diffusion models beat gans on image synthesis. In
250 Marc’Aurelio Ranzato, Alina Beygelzimer, Yann N. Dauphin, Percy Liang, and Jennifer Wortman
251 Vaughan, editors, *Advances in Neural Information Processing Systems 34: Annual Conference*
252 *on Neural Information Processing Systems 2021, NeurIPS 2021, December 6-14, 2021, virtual*,
253 pages 8780–8794, 2021. URL <https://proceedings.neurips.cc/paper/2021/hash/49ad23d1ec9fa4bd8d77d02681df5cfa-Abstract.html>.
254
- 255 Kyle D. Doherty, Marirose P. Kuhlman, Rebecca A. Durham, Philip W. Ramsey, and Daniel L.
256 Mummey. Fine-grained topographic diversity data improve site prioritization outcomes for
257 bees. *Ecological Indicators*, 132:108315, 2021. ISSN 1470-160X. doi: <https://doi.org/10.1016/j.ecolind.2021.108315>. URL <https://www.sciencedirect.com/science/article/pii/S1470160X21009808>.
258
259
- 260 Mark Everingham, Luc Van Gool, Christopher K. I. Williams, John Winn, and Andrew Zisserman.
261 The pascal visual object classes (voc) challenge. *International Journal of Computer Vision*, 88:303–
262 308, September 2009. URL <https://www.microsoft.com/en-us/research/publication/the-pascal-visual-object-classes-voc-challenge/>. Printed version publication date:
263 June 2010.
264
- 265 Li Fei-Fei, R. Fergus, and P. Perona. Learning generative visual models from few training examples:
266 An incremental bayesian approach tested on 101 object categories. In *2004 Conference on*
267 *Computer Vision and Pattern Recognition Workshop*, pages 178–178, 2004. doi: 10.1109/CVPR.
268 2004.383.
- 269 Rinon Gal, Yuval Alaluf, Yuval Atzmon, Or Patashnik, Amit H. Bermano, Gal Chechik, and Daniel
270 Cohen-Or. An image is worth one word: Personalizing text-to-image generation using textual
271 inversion, 2022. URL <https://arxiv.org/abs/2208.01618>.
- 272 Rohit Gandikota, Joanna Materzynska, Jaden Fiotto-Kaufman, and David Bau. Erasing concepts
273 from diffusion models. *CoRR*, abs/2303.07345, 2023. doi: 10.48550/arXiv.2303.07345. URL
274 <https://doi.org/10.48550/arXiv.2303.07345>.
- 275 Ian Goodfellow, Jean Pouget-Abadie, Mehdi Mirza, Bing Xu, David Warde-Farley, Sherjil Ozair,
276 Aaron Courville, and Yoshua Bengio. Generative adversarial nets. In Z. Ghahramani, M. Welling,
277 C. Cortes, N. Lawrence, and K.Q. Weinberger, editors, *Advances in Neural Information Processing*
278 *Systems*, volume 27. Curran Associates, Inc., 2014. URL <https://proceedings.neurips.cc/paper/2014/file/5ca3e9b122f61f8f06494c97b1afccf3-Paper.pdf>.
279
- 280 Ayaan Haque. EC-GAN: low-sample classification using semi-supervised algorithms and gans
281 (student abstract). In *Thirty-Fifth AAAI Conference on Artificial Intelligence, AAAI 2021, Thirty-*
282 *Third Conference on Innovative Applications of Artificial Intelligence, IAAI 2021, The Eleventh*
283 *Symposium on Educational Advances in Artificial Intelligence, EAAI 2021, Virtual Event, February*
284 *2-9, 2021*, pages 15797–15798. AAAI Press, 2021. URL <https://ojs.aaai.org/index.php/AAAI/article/view/17895>.
285
- 286 Ruifei He, Shuyang Sun, Xin Yu, Chuhui Xue, Wenqing Zhang, Philip Torr, Song Bai, and Xiaojuan
287 Qi. Is synthetic data from generative models ready for image recognition?, 2022. URL <https://arxiv.org/abs/2210.07574>.
288
- 289 Amir Hertz, Ron Mokady, Jay Tenenbaum, Kfir Aberman, Yael Pritch, and Daniel Cohen-Or. Prompt-
290 to-prompt image editing with cross attention control, 2022. URL <https://arxiv.org/abs/2208.01626>.
291
- 292 Jonathan Ho and Tim Salimans. Classifier-free diffusion guidance, 2022. URL <https://arxiv.org/abs/2207.12598>.
293
- 294 Jonathan Ho, Ajay Jain, and Pieter Abbeel. Denoising diffusion probabilistic models. In
295 Hugo Larochelle, Marc’Aurelio Ranzato, Raia Hadsell, Maria-Florina Balcan, and Hsuan-
296 Tien Lin, editors, *Advances in Neural Information Processing Systems 33: Annual Conference*
297 *on Neural Information Processing Systems 2020, NeurIPS 2020, December 6-*
298 *12, 2020, virtual*, 2020. URL <https://proceedings.neurips.cc/paper/2020/hash/4c5bcfec8584af0d967f1ab10179ca4b-Abstract.html>.
299

- 300 Ali Jahanian, Xavier Puig, Yonglong Tian, and Phillip Isola. Generative models as a data source
301 for multiview representation learning. In *The Tenth International Conference on Learning*
302 *Representations, ICLR 2022, Virtual Event, April 25-29, 2022*. OpenReview.net, 2022. URL
303 <https://openreview.net/forum?id=qhAeZjs7dCL>.
- 304 Diederik P. Kingma and Max Welling. Auto-encoding variational bayes. In Yoshua Bengio and Yann
305 LeCun, editors, *2nd International Conference on Learning Representations, ICLR 2014, Banff,*
306 *AB, Canada, April 14-16, 2014, Conference Track Proceedings*, 2014. URL [http://arxiv.org/](http://arxiv.org/abs/1312.6114)
307 [abs/1312.6114](http://arxiv.org/abs/1312.6114).
- 308 Jonathan Krause, Michael Stark, Jia Deng, and Li Fei-Fei. 3d object representations for fine-grained
309 categorization. In *2013 IEEE International Conference on Computer Vision Workshops*, pages
310 554–561, 2013. doi: 10.1109/ICCVW.2013.77.
- 311 Alina Kuznetsova, Hassan Rom, Neil Alldrin, Jasper R. R. Uijlings, Ivan Krasin, Jordi Pont-Tuset,
312 Shahab Kamali, Stefan Popov, Matteo Mallocci, Tom Duerig, and Vittorio Ferrari. The open images
313 dataset V4: unified image classification, object detection, and visual relationship detection at scale.
314 *CoRR*, abs/1811.00982, 2018. URL <http://arxiv.org/abs/1811.00982>.
- 315 Xiang Lisa Li and Percy Liang. Prefix-tuning: Optimizing continuous prompts for generation.
316 In Chengqing Zong, Fei Xia, Wenjie Li, and Roberto Navigli, editors, *Proceedings of the 59th*
317 *Annual Meeting of the Association for Computational Linguistics and the 11th International Joint*
318 *Conference on Natural Language Processing, ACL/IJCNLP 2021, (Volume 1: Long Papers), Virtual*
319 *Event, August 1-6, 2021*, pages 4582–4597. Association for Computational Linguistics, 2021.
320 doi: 10.18653/v1/2021.acl-long.353. URL [https://doi.org/10.18653/v1/2021.acl-long.](https://doi.org/10.18653/v1/2021.acl-long.353)
321 [353](https://doi.org/10.18653/v1/2021.acl-long.353).
- 322 Tsung-Yi Lin, Michael Maire, Serge J. Belongie, James Hays, Pietro Perona, Deva Ramanan, Piotr
323 Dollár, and C. Lawrence Zitnick. Microsoft COCO: common objects in context. In David J.
324 Fleet, Tomás Pajdla, Bernt Schiele, and Tinne Tuytelaars, editors, *Computer Vision - ECCV 2014*
325 *- 13th European Conference, Zurich, Switzerland, September 6-12, 2014, Proceedings, Part V*,
326 volume 8693 of *Lecture Notes in Computer Science*, pages 740–755. Springer, 2014. doi: 10.1007/
327 [978-3-319-10602-1_48](https://doi.org/10.1007/978-3-319-10602-1_48). URL https://doi.org/10.1007/978-3-319-10602-1_48.
- 328 Andreas Lugmayr, Martin Danelljan, Andrés Romero, Fisher Yu, Radu Timofte, and Luc Van Gool.
329 Repaint: Inpainting using denoising diffusion probabilistic models. In *IEEE/CVF Conference*
330 *on Computer Vision and Pattern Recognition, CVPR 2022, New Orleans, LA, USA, June 18-24,*
331 *2022*, pages 11451–11461. IEEE, 2022. doi: 10.1109/CVPR52688.2022.01117. URL <https://doi.org/10.1109/CVPR52688.2022.01117>.
- 333 S. Maji, J. Kannala, E. Rahtu, M. Blaschko, and A. Vedaldi. Fine-grained visual classification of
334 aircraft. Technical report, 2013.
- 335 Chenlin Meng, Yutong He, Yang Song, Jiaming Song, Jiajun Wu, Jun-Yan Zhu, and Stefano Ermon.
336 Sdedit: Guided image synthesis and editing with stochastic differential equations. In *The Tenth*
337 *International Conference on Learning Representations, ICLR 2022, Virtual Event, April 25-29,*
338 *2022*. OpenReview.net, 2022. URL https://openreview.net/forum?id=aBsCjcPu_tE.
- 339 Ron Mokady, Amir Hertz, Kfir Aberman, Yael Pritch, and Daniel Cohen-Or. Null-text inversion for
340 editing real images using guided diffusion models, 2022. URL [https://arxiv.org/abs/2211.](https://arxiv.org/abs/2211.09794)
341 [09794](https://arxiv.org/abs/2211.09794).
- 342 Alexander Quinn Nichol and Prafulla Dhariwal. Improved denoising diffusion probabilistic models.
343 In Marina Meila and Tong Zhang, editors, *Proceedings of the 38th International Conference on*
344 *Machine Learning, ICML 2021, 18-24 July 2021, Virtual Event*, volume 139 of *Proceedings of*
345 *Machine Learning Research*, pages 8162–8171. PMLR, 2021. URL [http://proceedings.mlr.](http://proceedings.mlr.press/v139/nichol21a.html)
346 [press/v139/nichol21a.html](http://proceedings.mlr.press/v139/nichol21a.html).
- 347 Alexander Quinn Nichol, Prafulla Dhariwal, Aditya Ramesh, Pranav Shyam, Pamela Mishkin, Bob
348 McGrew, Ilya Sutskever, and Mark Chen. GLIDE: towards photorealistic image generation and
349 editing with text-guided diffusion models. In Kamalika Chaudhuri, Stefanie Jegelka, Le Song,
350 Csaba Szepesvári, Gang Niu, and Sivan Sabato, editors, *International Conference on Machine*

- 351 *Learning, ICML 2022, 17-23 July 2022, Baltimore, Maryland, USA*, volume 162 of *Proceedings of*
352 *Machine Learning Research*, pages 16784–16804. PMLR, 2022. URL [https://proceedings.](https://proceedings.mlr.press/v162/nichol22a.html)
353 [mlr.press/v162/nichol22a.html](https://proceedings.mlr.press/v162/nichol22a.html).
- 354 Maria-Elena Nilsback and Andrew Zisserman. Automated flower classification over a large number
355 of classes. In *Indian Conference on Computer Vision, Graphics and Image Processing*, Dec 2008.
- 356 Luis Perez and Jason Wang. The effectiveness of data augmentation in image classification using
357 deep learning, 2017. URL <https://arxiv.org/abs/1712.04621>.
- 358 Aditya Ramesh, Prafulla Dhariwal, Alex Nichol, Casey Chu, and Mark Chen. Hierarchical text-
359 conditional image generation with clip latents, 2022. URL [https://arxiv.org/abs/2204.](https://arxiv.org/abs/2204.06125)
360 [06125](https://arxiv.org/abs/2204.06125).
- 361 Ali Razavi, Aäron van den Oord, and Oriol Vinyals. Generating diverse high-fidelity images with
362 VQ-VAE-2. In Hanna M. Wallach, Hugo Larochelle, Alina Beygelzimer, Florence d’Alché-Buc,
363 Emily B. Fox, and Roman Garnett, editors, *Advances in Neural Information Processing Systems*
364 *32: Annual Conference on Neural Information Processing Systems 2019, NeurIPS 2019, December*
365 *8-14, 2019, Vancouver, BC, Canada*, pages 14837–14847, 2019. URL [https://proceedings.](https://proceedings.neurips.cc/paper/2019/hash/5f8e2fa1718d1bbcadf1cd9c7a54fb8c-Abstract.html)
366 [neurips.cc/paper/2019/hash/5f8e2fa1718d1bbcadf1cd9c7a54fb8c-Abstract.html](https://proceedings.neurips.cc/paper/2019/hash/5f8e2fa1718d1bbcadf1cd9c7a54fb8c-Abstract.html).
- 367 Robin Rombach, Andreas Blattmann, Dominik Lorenz, Patrick Esser, and Björn Ommer. High-
368 resolution image synthesis with latent diffusion models. In *IEEE/CVF Conference on Computer*
369 *Vision and Pattern Recognition, CVPR 2022, New Orleans, LA, USA, June 18-24, 2022*, pages
370 10674–10685. IEEE, 2022. doi: 10.1109/CVPR52688.2022.01042. URL [https://doi.org/10.](https://doi.org/10.1109/CVPR52688.2022.01042)
371 [1109/CVPR52688.2022.01042](https://doi.org/10.1109/CVPR52688.2022.01042).
- 372 Chitwan Saharia, William Chan, Huiwen Chang, Chris A. Lee, Jonathan Ho, Tim Salimans, David J.
373 Fleet, and Mohammad Norouzi. Palette: Image-to-image diffusion models. In Munkhtsetseg
374 Nandigjav, Niloy J. Mitra, and Aaron Hertzmann, editors, *SIGGRAPH ’22: Special Interest*
375 *Group on Computer Graphics and Interactive Techniques Conference, Vancouver, BC, Canada,*
376 *August 7 - 11, 2022*, pages 15:1–15:10. ACM, 2022a. doi: 10.1145/3528233.3530757. URL
377 <https://doi.org/10.1145/3528233.3530757>.
- 378 Chitwan Saharia, William Chan, Saurabh Saxena, Lala Li, Jay Whang, Emily Denton, Seyed
379 Kamyar Seyed Ghasemipour, Burcu Karagol Ayan, S. Sara Mahdavi, Rapha Gontijo Lopes, Tim
380 Salimans, Jonathan Ho, David J Fleet, and Mohammad Norouzi. Photorealistic text-to-image
381 diffusion models with deep language understanding, 2022b. URL [https://arxiv.org/abs/](https://arxiv.org/abs/2205.11487)
382 [2205.11487](https://arxiv.org/abs/2205.11487).
- 383 Christoph Schuhmann, Romain Beaumont, Richard Vencu, Cade Gordon, Ross Wightman, Mehdi
384 Cherti, Theo Coombes, Aarush Katta, Clayton Mullis, Mitchell Wortsman, Patrick Schramowski,
385 Srivatsa Kundurthy, Katherine Crowson, Ludwig Schmidt, Robert Kaczmarczyk, and Jenia Jitsev.
386 Laion-5b: An open large-scale dataset for training next generation image-text models, 2022. URL
387 <https://arxiv.org/abs/2210.08402>.
- 388 Connor Shorten and Taghi M. Khoshgoftaar. A survey on image data augmentation for deep learning.
389 *Journal of Big Data*, 6(1):60, Jul 2019. ISSN 2196-1115. doi: 10.1186/s40537-019-0197-0. URL
390 <https://doi.org/10.1186/s40537-019-0197-0>.
- 391 Jascha Sohl-Dickstein, Eric A. Weiss, Niru Maheswaranathan, and Surya Ganguli. Deep unsupervised
392 learning using nonequilibrium thermodynamics. In Francis R. Bach and David M. Blei, editors,
393 *Proceedings of the 32nd International Conference on Machine Learning, ICML 2015, Lille, France,*
394 *6-11 July 2015*, volume 37 of *JMLR Workshop and Conference Proceedings*, pages 2256–2265.
395 JMLR.org, 2015. URL <http://proceedings.mlr.press/v37/sohl-dickstein15.html>.
- 396 Jiaming Song, Chenlin Meng, and Stefano Ermon. Denoising diffusion implicit models. In *9th*
397 *International Conference on Learning Representations, ICLR 2021, Virtual Event, Austria, May*
398 *3-7, 2021*. OpenReview.net, 2021. URL <https://openreview.net/forum?id=St1giarCHLP>.
- 399 Chen Sun, Abhinav Shrivastava, Saurabh Singh, and Abhinav Gupta. Revisiting unreasonable
400 effectiveness of data in deep learning era. In *IEEE International Conference on Computer Vision,*
401 *ICCV 2017, Venice, Italy, October 22-29, 2017*, pages 843–852. IEEE Computer Society, 2017.
402 doi: 10.1109/ICCV.2017.97. URL <https://doi.org/10.1109/ICCV.2017.97>.

- 403 Fabio Henrique Kiyoi dos Santos Tanaka and Claus Aranha. Data augmentation using gans, 2019.
404 URL <https://arxiv.org/abs/1904.09135>.
- 405 Hugo Touvron, Matthieu Cord, Matthijs Douze, Francisco Massa, Alexandre Sablayrolles, and Hervé
406 Jégou. Training data-efficient image transformers & distillation through attention. In Marina Meila
407 and Tong Zhang, editors, *Proceedings of the 38th International Conference on Machine Learning,*
408 *ICML 2021, 18-24 July 2021, Virtual Event*, volume 139 of *Proceedings of Machine Learning*
409 *Research*, pages 10347–10357. PMLR, 2021. URL [http://proceedings.mlr.press/v139/](http://proceedings.mlr.press/v139/touvron21a.html)
410 [touvron21a.html](http://proceedings.mlr.press/v139/touvron21a.html).
- 411 Toan Tran, Trung Pham, Gustavo Carneiro, Lyle J. Palmer, and Ian D. Reid. A bayesian data
412 augmentation approach for learning deep models. In Isabelle Guyon, Ulrike von Luxburg,
413 Samy Bengio, Hanna M. Wallach, Rob Fergus, S. V. N. Vishwanathan, and Roman Gar-
414 nett, editors, *Advances in Neural Information Processing Systems 30: Annual Conference on*
415 *Neural Information Processing Systems 2017, December 4-9, 2017, Long Beach, CA, USA*,
416 pages 2797–2806, 2017. URL [https://proceedings.neurips.cc/paper/2017/hash/](https://proceedings.neurips.cc/paper/2017/hash/076023edc9187cf1ac1f1163470e479a-Abstract.html)
417 [076023edc9187cf1ac1f1163470e479a-Abstract.html](https://proceedings.neurips.cc/paper/2017/hash/076023edc9187cf1ac1f1163470e479a-Abstract.html).
- 418 Sajila Wickramaratne and Md Shaad Mahmud. Conditional-gan based data augmentation for deep
419 learning task classifier improvement using fnirs data. *Frontiers in Big Data*, 4:659146, 07 2021.
420 doi: 10.3389/fdata.2021.659146.
- 421 Wei Xiong, Yutong He, Yixuan Zhang, Wenhan Luo, Lin Ma, and Jiebo Luo. Fine-grained image-to-
422 image transformation towards visual recognition. In *Proceedings of the IEEE/CVF Conference on*
423 *Computer Vision and Pattern Recognition (CVPR)*, June 2020.
- 424 Shin’ya Yamaguchi, Sekitoshi Kanai, and Takeharu Eda. Effective data augmentation with multi-
425 domain learning gans. In *The Thirty-Fourth AAAI Conference on Artificial Intelligence, AAAI*
426 *2020, The Thirty-Second Innovative Applications of Artificial Intelligence Conference, IAAI*
427 *2020, The Tenth AAAI Symposium on Educational Advances in Artificial Intelligence, EAAI*
428 *2020, New York, NY, USA, February 7-12, 2020*, pages 6566–6574. AAAI Press, 2020. URL
429 <https://ojs.aaai.org/index.php/AAAI/article/view/6131>.
- 430 Xiaohui Yang, Anne M. Smith, Robert S. Bouchier, Kim Hodge, and Dustin Ostrander. Flowering
431 leafy spurge (*euphorbia esula*) detection using unmanned aerial vehicle imagery in biological
432 control sites: Impacts of flight height, flight time and detection method. *Weed Technology*, 34(4):
433 575–588, 2020. doi: 10.1017/wet.2020.8.
- 434 Sangdoon Yun, Dongyoon Han, Sanghyuk Chun, Seong Joon Oh, Youngjoon Yoo, and Junsuk Choe.
435 Cutmix: Regularization strategy to train strong classifiers with localizable features. In *2019*
436 *IEEE/CVF International Conference on Computer Vision, ICCV 2019, Seoul, Korea (South),*
437 *October 27 - November 2, 2019*, pages 6022–6031. IEEE, 2019. doi: 10.1109/ICCV.2019.00612.
438 URL <https://doi.org/10.1109/ICCV.2019.00612>.
- 439 Xiaohua Zhai, Joan Puigcerver, Alexander Kolesnikov, Pierre Ruysen, Carlos Riquelme, Mario
440 Lucic, Josip Djolonga, André Susano Pinto, Maxim Neumann, Alexey Dosovitskiy, Lucas Beyer,
441 Olivier Bachem, Michael Tschannen, Marcin Michalski, Olivier Bousquet, Sylvain Gelly, and
442 Neil Houlsby. The visual task adaptation benchmark. *CoRR*, abs/1910.04867, 2019. URL
443 <http://arxiv.org/abs/1910.04867>.
- 444 Yuxuan Zhang, Wenzheng Chen, Huan Ling, Jun Gao, Yinan Zhang, Antonio Torralba, and Sanja
445 Fidler. Image gans meet differentiable rendering for inverse graphics and interpretable 3d neural
446 rendering. In *9th International Conference on Learning Representations, ICLR 2021, Virtual Event,*
447 *Austria, May 3-7, 2021*. OpenReview.net, 2021a. URL [https://openreview.net/forum?id=](https://openreview.net/forum?id=yWkP7JuHX1)
448 [yWkP7JuHX1](https://openreview.net/forum?id=yWkP7JuHX1).
- 449 Yuxuan Zhang, Huan Ling, Jun Gao, Kangxue Yin, Jean-Francois Lafleche, Adela Bar-
450 riuoso, Antonio Torralba, and Sanja Fidler. Datasetgan: Efficient labeled data factory
451 with minimal human effort. In *IEEE Conference on Computer Vision and Pattern*
452 *Recognition, CVPR 2021, virtual, June 19-25, 2021*, pages 10145–10155. Computer Vi-
453 sion Foundation / IEEE, 2021b. doi: 10.1109/CVPR46437.2021.01001. URL [https://](https://openaccess.thecvf.com/content/CVPR2021/html/Zhang_DatasetGAN_Efficient_Labeled_Data_Factory_With_Minimal_Human_Effort_CVPR_2021_paper.html)
454 [openaccess.thecvf.com/content/CVPR2021/html/Zhang_DatasetGAN_Efficient_](https://openaccess.thecvf.com/content/CVPR2021/html/Zhang_DatasetGAN_Efficient_Labeled_Data_Factory_With_Minimal_Human_Effort_CVPR_2021_paper.html)
455 [Labeled_Data_Factory_With_Minimal_Human_Effort_CVPR_2021_paper.html](https://openaccess.thecvf.com/content/CVPR2021/html/Zhang_DatasetGAN_Efficient_Labeled_Data_Factory_With_Minimal_Human_Effort_CVPR_2021_paper.html).

- 456 Shengyu Zhao, Zhijian Liu, Ji Lin, Jun-Yan Zhu, and Song Han. Differentiable augmentation for
457 data-efficient GAN training. In Hugo Larochelle, Marc’Aurelio Ranzato, Raia Hadsell, Maria-
458 Florina Balcan, and Hsuan-Tien Lin, editors, *Advances in Neural Information Processing Systems*
459 *33: Annual Conference on Neural Information Processing Systems 2020, NeurIPS 2020, December*
460 *6-12, 2020, virtual*, 2020. URL [https://proceedings.neurips.cc/paper/2020/hash/
461 55479c55ebd1efd3ff125f1337100388-Abstract.html](https://proceedings.neurips.cc/paper/2020/hash/55479c55ebd1efd3ff125f1337100388-Abstract.html).
- 462 Zhedong Zheng, Liang Zheng, and Yi Yang. Unlabeled samples generated by GAN improve the
463 person re-identification baseline in vitro. In *IEEE International Conference on Computer Vision,*
464 *ICCV 2017, Venice, Italy, October 22-29, 2017*, pages 3774–3782. IEEE Computer Society, 2017.
465 doi: 10.1109/ICCV.2017.405. URL <https://doi.org/10.1109/ICCV.2017.405>.

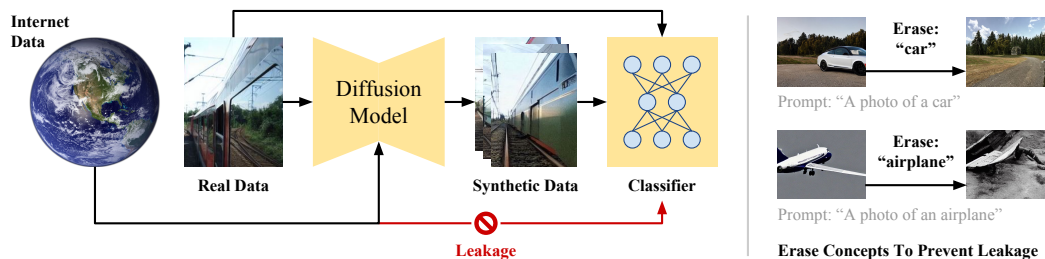


Figure 8: Leakage of internet data to downstream models. Large generative models trained at internet scale may produce synthetic data similar to their training data when tested on common concepts (right). We show the result of erasing common concepts by fine-tuning the attention layer weights of Stable Diffusion’s UNet (right).

466 A Data Preparation

467 **Standard Datasets** We benchmark our data augmentations on six standard computer vision datasets.
 468 We employ Caltech101 [Fei-Fei et al., 2004], Flowers102 [Nilsback and Zisserman, 2008], FGVC
 469 Aircraft [Maji et al., 2013], Stanford Cars [Krause et al., 2013], COCO Lin et al. [2014], and PASCAL
 470 VOC Everingham et al. [2009]. We use the official 2017 training and validation sets of COCO, and
 471 the official 2012 training and validation sets of PASCAL VOC. We adapt these datasets into object
 472 classification tasks by filtering images that have at least one object segmentation mask. We assign
 473 these images labels corresponding to the class of object with largest area in the image, as measured by
 474 the pixels contained in the mask. Caltech101, COCO, and PASCAL VOC have *common* concepts like
 475 "dog" and Flowers102, FGVC Aircraft, and Stanford Cars have *fine-grain* concepts like "giant white
 476 arum lily" (the specific flower name). Additional details for preparing datasets are in Appendix K.

477 **Leafy Spurge** We contribute a dataset of top-
 478 down drone images of semi-natural areas in the
 479 western United States. These data were gathered
 480 in an effort to better map the extent of a prob-
 481 lematic invasive plant, leafy spurge (*Euphorbia*
 482 *esula*), that is a detriment to natural and agricul-
 483 tural ecosystems in temperate regions of North
 484 America. Prior work to classify aerial imagery
 485 of leafy spurge achieved an accuracy of 0.75
 486 Yang et al. [2020]. To our knowledge, top-down
 487 aerial imagery of leafy spurge was not present
 488 in the Stable Diffusion training data. Results of
 489 CLIP-retrieval Beaumont [2022] returned close-up,
 490 side-on images of members of the same genus
 491 (Figure 9) in the top 20 results. We observed the first instance of our target species, *Euphorbia*
 492 *esula*, as a 35th result. The spurge images we contribute are semantically distinct from those in the
 493 CLIP corpus, because they capture the plant and landscape context around it from 50m distance
 494 above the ground, rather than close-up botanical features. Therefore, this dataset represents a unique
 495 opportunity to explore few-shot learning with Stable Diffusion, and developing a robust classifier
 would directly benefit efforts to restore natural ecosystems. Additional details are in Appendix L.



Figure 9: A sample from the Spurge dataset (the first on the left), compared with top results of CLIP-retrieval queried on the prompt: "a drone image of leafy spurge". Closeup images from members of the same genus (second, and third) are in the top 20 results and a closeup of the same species for the 35th result (fourth). No top-down aerial images of the target plant were revealed.

496 B Related Work

497 Generative models have been the subject of growing interest and rapid advancement. Earlier methods,
 498 including VAEs Kingma and Welling [2014] and GANs Goodfellow et al. [2014], showed initial
 499 promise generating realistic images, and were scaled up in terms of resolution and sample quality
 500 Brock et al. [2019], Razavi et al. [2019]. Despite the power of these methods, many recent successes
 501 in photorealistic image generation were the result of diffusion models Ho et al. [2020], Nichol
 502 and Dhariwal [2021], Saharia et al. [2022b], Nichol et al. [2022], Ramesh et al. [2022]. Diffusion
 503 models have been shown to generate higher-quality samples compared to their GAN counterparts
 504 Dhariwal and Nichol [2021], and developments like classifier free guidance Ho and Salimans [2022]
 505 have made text-to-image generation possible. Recent emphasis has been on training these models
 506 with internet-scale datasets like LAION-5B Schuhmann et al. [2022]. Generative models trained

507 at internet-scale Rombach et al. [2022], Saharia et al. [2022b], Nichol et al. [2022], Ramesh et al.
508 [2022] have unlocked several application areas where photorealistic generation is crucial.

509 **Image Editing** Diffusion models have popularized image-editing. Inpainting with diffusion is one
510 such approach that allows the user to specify what to edit as a mask Saharia et al. [2022a], Lugmayr
511 et al. [2022]. Other works avoid masks and modify the attention weights of the diffusion process
512 that generated the image instead Hertz et al. [2022], Mokady et al. [2022]. Perhaps the most relevant
513 technique to our work is SDEdit Meng et al. [2022], where real images are inserted partway through
514 the reverse diffusion process. SDEdit is applied by He et al. [2022] to generate synthetic data for
515 training classifiers, but our analysis differs from theirs in that we study generalization to new concepts
516 the diffusion model wasn’t trained on. To instruct the diffusion model on what to augment, we
517 optimize a pseudo-prompt [Li and Liang, 2021, Gal et al., 2022] for each concept. Our strategy is
518 more appealing than fine-tuning the whole model as in Azizi et al. [2023] since it works from just one
519 example per concept (Azizi et al. [2023] require millions of images), and doesn’t disturb the model’s
520 ability to generate other concepts. Our fine-tuning strategy improves the quality of augmentations for
521 common concepts Stable Diffusion has seen, and for fine-grain concepts that are less common.

522 **Synthetic Data** Training neural networks on synthetic data from generative models was popularized
523 using GANs Antoniou et al. [2017], Tran et al. [2017], Zheng et al. [2017]. Various applications for
524 synthetic data generated from GANs have been studied, including representation learning Jahanian
525 et al. [2022], inverse graphics Zhang et al. [2021a], semantic segmentation Zhang et al. [2021b], and
526 training classifiers Tanaka and Aranha [2019], Dat et al. [2019], Yamaguchi et al. [2020], Besnier
527 et al. [2020], Xiong et al. [2020], Wickramaratne and Mahmud [2021], Haque [2021]. More recently,
528 synthetic data from diffusion models has also been studied in a few-shot setting He et al. [2022].
529 These works use generative models that have likely seen images of target classes and, to the best of
530 our knowledge, we present the first analysis for synthetic data on previously unseen concepts.

531 C Background

532 Diffusion models Sohl-Dickstein et al. [2015], Ho et al. [2020], Nichol and Dhariwal [2021], Song
533 et al. [2021], Rombach et al. [2022] are sequential latent variable models inspired by thermodynamic
534 diffusion Sohl-Dickstein et al. [2015]. They generate samples via a Markov chain with learned
535 Gaussian transitions starting from an initial noise distribution $p(x_T) = \mathcal{N}(x_T; 0, I)$.

$$p_\theta(x_{0:T}) = p(x_T) \prod_{t=1}^T p_\theta(x_{t-1}|x_t) \quad (4)$$

536 Transitions $p_\theta(x_{t-1}|x_t)$ are designed to gradually reduce variance according to a schedule β_1, \dots, β_T
537 so the final sample x_0 represents a sample from the true distribution. Transitions are often parameter-
538 ized by a fixed covariance $\Sigma_t = \beta_t I$ and a learned mean $\mu_\theta(x_t, t)$ defined below.

$$\mu_\theta(x_t, t) = \frac{1}{\sqrt{\alpha_t}} \left(x_t - \frac{\beta_t}{\sqrt{1 - \tilde{\alpha}_t}} \epsilon_\theta(x_t, t) \right) \quad (5)$$

539 This parameterization choice results from deriving the optimal reverse process Ho et al. [2020], where
540 $\epsilon_\theta(\cdot)$ is a neural network trained to process a noisy sample x_t and predict added noise. Given real
541 samples x_0 and noise $\epsilon \sim \mathcal{N}(0, I)$, one can derive x_t at an arbitrary timestep below.

$$x_t(x_0, \epsilon) = \sqrt{\tilde{\alpha}_t} x_0 + \sqrt{1 - \tilde{\alpha}_t} \epsilon \quad (6)$$

542 Ho et al. [2020] define $\alpha_t = 1 - \beta_t$ and $\tilde{\alpha}_t = \prod_{s=1}^t \alpha_s$. These components allow training and
543 sampling from the type of diffusion model backbone in this work. We use a pretrained Stable
544 Diffusion model trained by Rombach et al. [2022]. Among other differences, this model includes a
545 text encoder that enables text-to-image generation (refer to Appendix K for model details).

546 D Limitations & Safeguards

547 As generative models have improved in terms of fidelity and scale, they have been shown to occasion-
548 ally produce harmful content, including images that reinforce stereotypes, and images that include
549 nudity or violence. Synthetic data from generative models, when it suffers from these problems,
550 has the potential to increase bias in downstream classifiers trained on such images if not handled.

551 We employ two mitigation techniques to lower the risk of leakage of harmful content into our data
 552 augmentation strategy. First, we use a safety checker that determines whether augmented images
 553 contain nudity or violence. If they do, the generation is discarded and re-sampled until a clean image
 554 is returned. Second, rather than generate images from scratch, our method edits real images, and
 555 keeps the original high-level structure of the real images. In this way, we can guide the model away
 556 from harmful content by ensuring the real images contain no harmful content to begin with. The
 557 combination of these techniques lowers the risk of leakage of harmful content, but is not a perfect
 558 solution. In particular, detecting biased content that encourages racial or gender stereotypes that exist
 559 online is much harder than detecting nudity or violence, and one limitation of this work is that we
 560 can't yet defend against this. We emphasize the importance of curating unbiased and safe datasets for
 561 training large generative models, and the creation of post-training bias mitigation techniques.

562 E Ethical Considerations

563 There are potential ethical concerns arising from large-scale generative models. For example, these
 564 models have been trained on large amounts of user data from the internet without the explicit consent
 565 of these users. Since our data augmentation strategy employs Stable Diffusion [Rombach et al., 2022],
 566 our method has the potential to generate augmentations that resemble or even copy data from such
 567 users online. This issue is not specific to our work; rather, it is inherent to image generation models
 568 trained at scales as large as Stable Diffusion, and other works using Stable Diffusion also face this
 569 ethical problem. Our mitigation to this ethical problem is to allow deletion of concepts from the
 570 weights of Stable Diffusion before augmentation. Deletion removes harmful, or copyrighted material
 571 from Stable Diffusion weights to ensure it cannot be copied by the model during augmentation.

572 F Broader Impacts

573 Data augmentation strategies like DA-Fusion have the potential to enable
 574 training vision models of a variety of
 575 types from limited data. While we
 576 studied classification in this work, DA-
 577 Fusion may also be applied to video
 578 classification, object detection, and
 579 visual reinforcement learning. One
 580 risk associated with improved few-
 581 shot learning on vision-based tasks
 582 is that synthetic data can be generated
 583 targeting particular users. For exam-
 584 ple, suppose one intends to build a
 585 person-identification system used to
 586 record the behavior patterns of a spec-
 587 ific person in public. Such a system
 588 trained with generative model-based data
 589 augmentations may only need one real
 590 photo to be trained. This poses a risk
 591 to privacy, despite other benefits that
 592 few-shot learning provides. As another
 593 example, suppose one intends to build
 594 a system capable of generating porno-
 595 graphy of a specific celebrity. Few-
 596 shot learning makes this possible with
 597 just a handful of real images that exist
 598 online. This poses a risk to personal
 599 safety and bodily autonomy of the
 600 targeted person.

594 G Additional Results

595 We conduct additional experiments on the Caltech101 [Fei-Fei et al., 2004], and Flowers102 [Nilsback
 596 and Zisserman, 2008] datasets, two standard image classification tasks for few-shot classification,
 597 which are in the Visual Task Adaptation Benchmark [Zhai et al., 2019]. Results in Figure 11 show
 598 that DA-Fusion improves classification performance both when using a model-centric defense against
 599 training data leakage, and a data-centric defense, described in Section 3.1 of the paper.

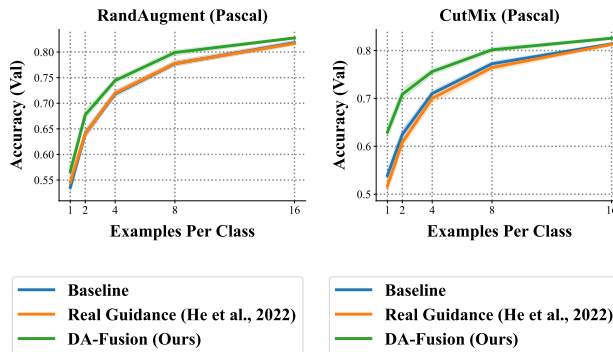


Figure 10: Results with stronger data-augmentation baselines. DA-Fusion improves over both RandAugment (using default PyTorch settings), and CutMix (with default setting from Yun et al. [2019]). Note that RandAugment results use model-centric leakage prevention, and CutMix results use data-centric leakage prevention, showing we improve over stronger baselines in both regimes.

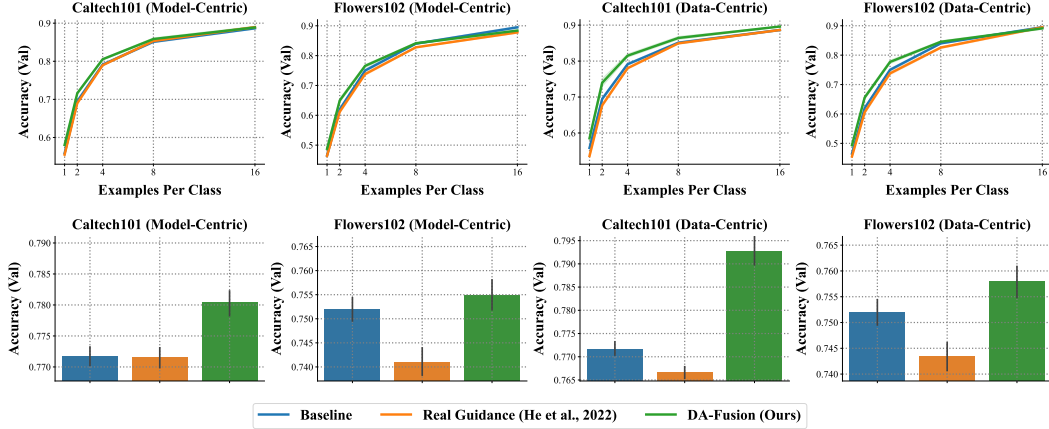
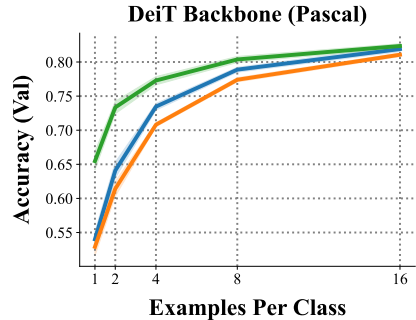


Figure 11: Few-shot classification performance with both kinds of leakage prevention on additional datasets. DA-Fusion outperforms the standard data augmentation baseline, and a competitive method from recent literature. These results reinforce the message in the main paper: DA-Fusion is an effective data augmentation strategy.

600 H Stronger Augmentation Baselines

601 In the main paper, we considered data augmentation base-
 602 lines consisting only of randomized rotations and flips. In
 603 this section, we compare against two stronger data aug-
 604 mentation methods: RandAugment [Cubuk et al., 2020],
 605 and CutMix [Yun et al., 2019]. Results are presented in
 606 Figure 10, and show that DA-Fusion improves over both
 607 RandAugment and CutMix on the Pascal-based task.



608 I Different Classifier Architectures

609 Results in the main paper use a ResNet50 architecture
 610 for the image classifier. In this section, we consider the
 611 Data-Efficient Image Transformer (DeiT) [Touvron et al.,
 612 2021], and evaluate DA-Fusion with data-centric leakage
 613 prevention on the Pascal task. Results in Figure 12 show
 614 that DA-Fusion improves the performance of DeiT, and
 615 suggests gains generalize to different architectures, includ-
 616 ing both convolution-based models (such as ResNet50),
 617 and attention-based ones (such as ViT).

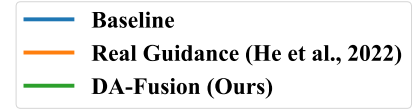


Figure 12: Few-shot results with a stronger classification model. DA-Fusion improves DeiT when compared to standard data augmentation baseline, and Real Guidance.

618 J Balancing Real & Synthetic Data

619 Training models on synthetic images often risks over-emphasizing spurious qualities and biases
 620 resulting from an imperfect generative model Antoniou et al. [2017]. The common solution assigns
 621 different sampling probabilities to real and synthetic images to manage imbalance He et al. [2022].
 622 We adopt a similar method for balancing real and synthetic data in Equation 7, where α denotes the
 623 probability that a synthetic image is present at the l -th location in the minibatch of images B .

$$i \sim \mathcal{U}(\{1, \dots, N\}), j \sim \mathcal{U}(\{1, \dots, M\}) \quad (7)$$

$$B_{l+1} \leftarrow B_l \cup \{X_i \text{ w.p. } (1 - \alpha) \text{ else } \tilde{X}_{ij}\} \quad (8)$$

624 Here $X \in \mathcal{R}^{N \times H \times W \times 3}$ denotes a dataset of N real images, and $i \in \mathbb{Z}$ specifies the index of a
 625 particular image X_i . For each image, we generate M augmentations, resulting in a synthetic dataset
 626 $\tilde{X} \in \mathcal{R}^{N \times M \times H \times W \times 3}$ with $N \times M$ image augmentations, where $\tilde{X}_{ij} \in \mathcal{R}^{H \times W \times 3}$ enumerates
 627 the j th augmentation for the i th image in the dataset. Indices i and j are sampled uniformly from

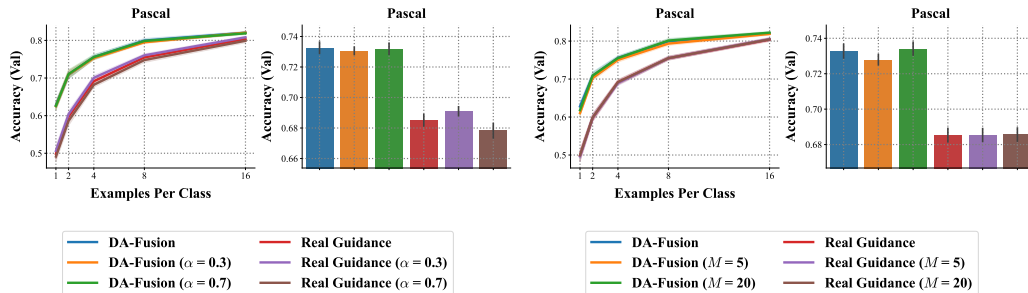


Figure 13: Ablation for data balance sensitivity. We run our method with $\alpha \in \{0.3, 0.5, 0.7\}$ and $M \in \{5, 10, 20\}$ and report the improvement in few-shot classification accuracy over Real Guidance using the same settings. DA-Fusion is robust to the balance of real and synthetic data and outperforms prior work in each setting.

628 the available N real images and their M augmented versions respectively. Given indices ij , with
 629 probability $(1 - \alpha)$ a real image image X_i is added to the batch B , otherwise its augmented image
 630 \tilde{X}_{ij} is added. Hyper-parameter details are presented in Appendix K, and we find $\alpha = 0.5$ to work
 631 effectively in all domains tested, which equally balances real and synthetic images.

632 J.1 DA-Fusion Is Robust To Data Balance

633 We next conduct an ablation to understand the sensitivity of our method to the balance of real and
 634 synthetic data, controlled by two hyperparameters: the number of synthetic images per real image
 635 $M \in \mathbb{N}$, and the probability of sampling synthetic images during training $\alpha \in [0, 1]$. We use $\alpha = 0.5$
 636 and $M = 10$ throughout the paper. Insensitivity to the particular value of α and M is a desirable
 637 trait because it simplifies hyper-parameter tuning and facilitates our data augmentation working
 638 out-of-the-box with no domain-specific tuning. We test sensitivity to α and M by comparing runs
 639 of DA-Fusion with different assignments to Real Guidance with the same α and M . Figure 13
 640 shows stability as α and M varies, and that $\alpha = 0.7$ performs marginally better than $\alpha = 0.5$, which
 641 suggests our method improves synthetic image quality because sampling them more often improves
 642 accuracy. While $M = 20$ performs marginally better than $M = 10$, the added cost of doubling the
 643 number of generative model calls for a marginal improvement suggests $M = 10$ is sufficient.

644 K Hyperparameters

645 Our method inherits the hyperparameters of text-to-image diffusion models and SDEdit Meng et al.
 646 [2022]. In addition, we introduce several other hyperparameters in this work that control the diversity
 647 of the synthetic images. Specific values for these hyperparameters are given in Table 1.

648 We uniformly at random select 20 classes per dataset for evaluation, turning them into 20-way
 649 classification tasks. This reduces the computational cost of reproducing the results in our paper, and
 650 the exact classes used in each dataset can be found in the open-source code.

651 L Leafy Spurge Dataset Acquisition and Pre-processing

652 In June 2022 botanists visited areas in western Montana, United States known to harbor leafy spurge
 653 and verified the presence or absence of the target plant at 39 sites. We selected sites that represented a
 654 range of elevation and solar input values as influenced by terrain. These environmental axes strongly
 655 drive variation in the structure and composition of vegetation Amatulli et al. [2018], Doherty et al.
 656 [2021]. Thus, stratifying by these aspects of the environment allowed us to test the performance of
 657 classifiers when presented with a diversity of plants which could be confused with our target.

658 During surveys, each site was divided into a 3×3 grid of plots that were 10m on side (**Fig. 14**),
 659 and then botanists confirmed the presence or absence of leafy spurge within each grid cell. After
 660 surveying we flew a DJI Phantom 4 Pro at 50m above the center of each site and gathered still RGB
 661 images. All images were gathered on the same day in the afternoon with sunny lighting conditions.

Hyperparameter Name	Value
Synthetic Probability α	0.5
Real Guidance Strength t_0	0.5
Num Intensities k	4
Intensities Distribution t_0	$\mathcal{U}(\{0.25, 0.5, 0.75, 1.0\})$
Synthetic Images Per Real M	10
Synthetic Images Per Real M (spurge)	50
Textual Inversion Token Initialization	"the"
Textual Inversion Batch Size	4
Textual Inversion Learning Rate	0.0005
Textual Inversion Training Steps	1000
Class Agnostic Prompt	"a photo"
Standard Prompt	"a photo of a <class name>"
Textual Inversion Prompt	"a photo of a ClassX"
Stable Diffusion Checkpoint	CompVis/stable-diffusion-v1-4
Stable Diffusion Guidance Scale	7.5
Stable Diffusion Resolution	512
Stable Diffusion Denoising Steps	1000
Classifier Architecture	ResNet50
Classifier Learning Rate	0.0001
Classifier Batch Size	32
Classifier Training Steps	10000
Classifier Early Stopping Interval	200

Table 1: Hyperparameters and their values.

662 We then cropped the the raw images to match the bounds of plots using visual markers installed
663 during surveys as guides (**Fig. 15**). Resulting crops varied in size because of the complexity of terrain.
664 E.G., ridges were closer to the drone sensor than valleys. Thus, image side lengths ranged from 533
665 to 1059 pixels. The mean side length was 717 and the mean spatial resolution, or ground sampling
666 distance, of pixels was 1.4 cm.

667 In our initial hyperparameter search we found that the classification accuracy of plot-scale images
668 was less than that of a classifier trained on smaller crops of the plots. Therefore, we generated four
669 250x250 pixel crops sharing a corner at plot centers for further experimentation (**Fig. 16**). Because
670 spurge plants were patchily distributed within a plot, a botanist reviewed each crop in the present
671 class and removed cases in which cropping resulted in samples where target plants were not visually
672 apparent.

673 M Benchmarking the Leafy Spurge Dataset

674 We benchmark classifier performance here on the full leafy spurge dataset, comparing a baseline
675 approach incorporating legacy augmentations with our novel DA-fusion method. For 15 trials we
676 generated random validation sets with 20 percent of the data, and fine-tuned a pretrained ResNet50
677 on the remaining 80 percent using the training hyperparameters reported in section ?? for 500 epochs.
678 From these trials we compute cross-validated mean accuracy and 68 percent confidence intervals.

679 In the case of baseline experiments, we augment data by flipping vertically and horizontally, as well as
680 randomly rotating by as much as 45 degrees with a probability of 0.5. For DA-Fusion augmentations
681 we take two approaches(**Fig. 17**) The first we refer to as DA-Fusion Pooled, and we apply the
682 methods of Textual Inversion Gal et al. [2022], but include all instances of a class in a single session
683 of fine-tuning, generating one token per class. In the second approach we refer to as DA-Fusion
684 Specific, we fine-tune and generate unique tokens for each image in the training set. In the specific
685 case, we generated 90, 180, and 270 rotations as well as horizontal and vertical flips and contribute
686 these along with original image for Stable Diffusion fine-tuning to achieve the target number of
687 images suggested to maximize performanceGal et al. [2022]. In both DA-Fusion approaches we
688 generated ten synthetic images per real image for model training. We maintain $\alpha = 0.5$, evenly
689 mixing real and synthetic data during training. We also maximize synthetic diversity by randomly

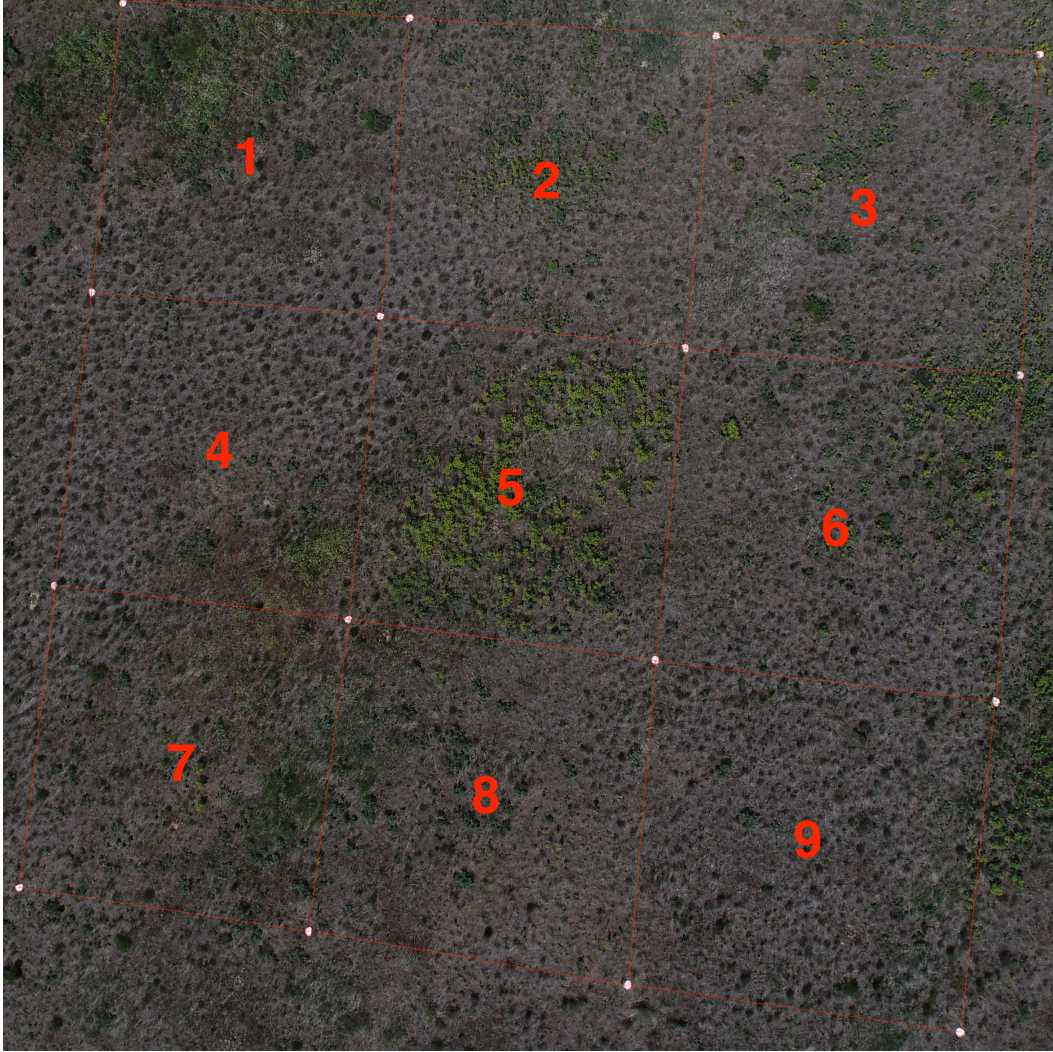


Figure 14: A drone image of surveyed areas containing leafy spurge. At each site botanists verified spurge presence or absence in a grid of nine spatially distinct plots. Note that cell five is rich in leafy spurge.

690 selecting 0.25, 0.5, 0.75, and 1.0 t_0 values. Note that we do not apply concept erasure here as in
691 few-shot experiments from the body text.

692 Both approaches to DA-Fusion offer slight performance enhancements over baseline augmentation
693 methods for the full leafy spurge dataset. We observe a 1.0% gain when applying DA-Fusion
694 Pooled and a 1.2% gain when applying DA-Fusion Specific(**Fig. 18**). It is important to note that, as
695 implemented currently, compute time for DA-Fusion Specific is linearly related to data amount, but
696 DA-Fusion Pooled compute is the same regardless of data size.

697 While pooling was not the most beneficial in this experiment, we support investigating it further.
698 This is because fine-tuning a leafy spurge token in a pooled approach might help to orient our target
699 in the embedding space where plants with similar diagnostic properties, such as flower shape and
700 color from the same genus, may be well represented. However, the leafy-spurge negative cases
701 do not correspond to a single semantic concept, but a plurality, such as green fields, brown fields,
702 and wooded areas. It is unclear if fine-tuning a single token for negative cases by a pooled method
703 would remove diversity from synthetic samples of spurge-free background landscapes, relative to
704 an image-specific approach. For this reason, we suspect a hybrid approach of pooled token for the
705 positive case and specific tokens for the negative cases could offer further gains, and support the
706 application of detecting weed invasions into new areas.

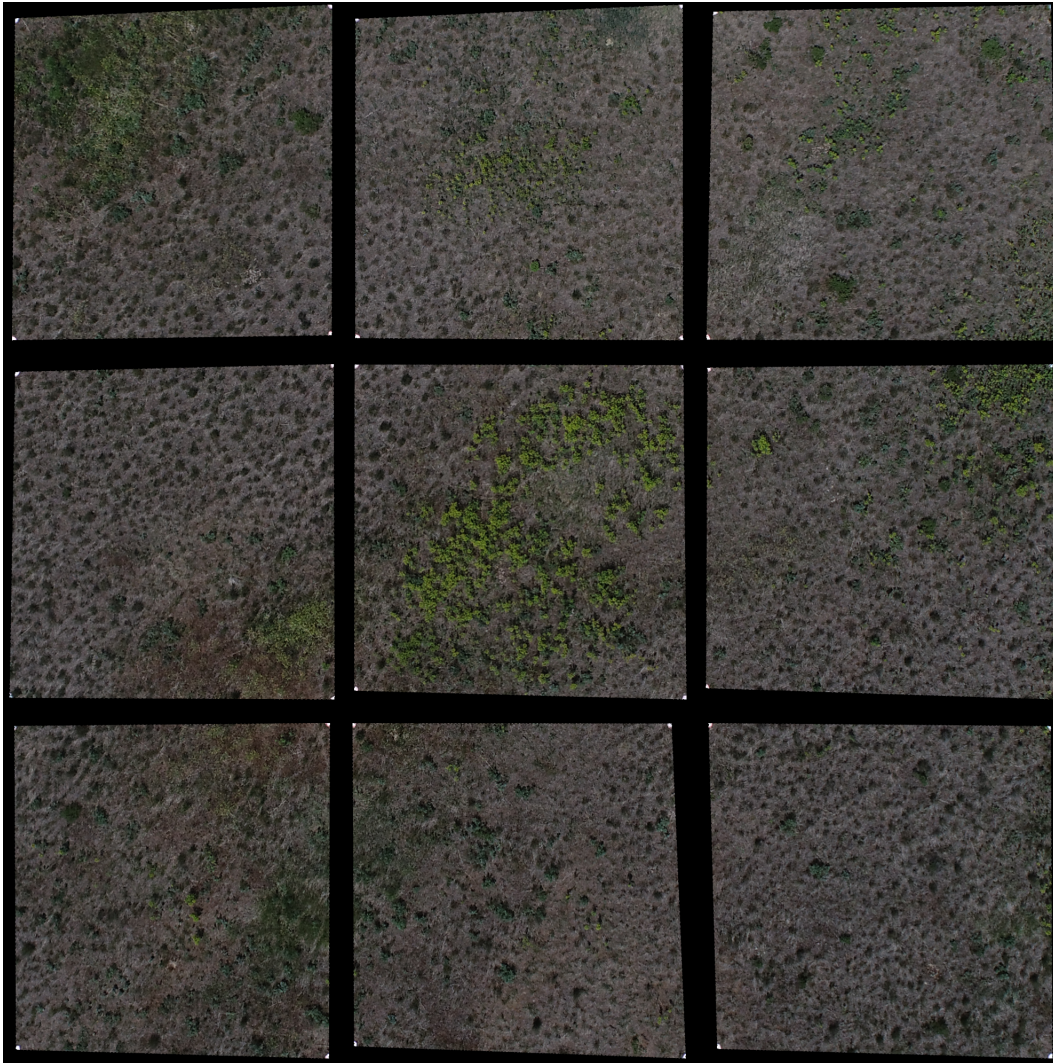


Figure 15: Markers installed at the corners of plots were used to crop plots from source images.



Figure 16: At each plot image center we cropped four 250x250 pixel sub-plots. We did this to amplify our data and improve classifier performance. The crops of plots with spurge present labels were inspected by a botanist to filter out examples where cropping excluded the target plant or the plants were not apparent.

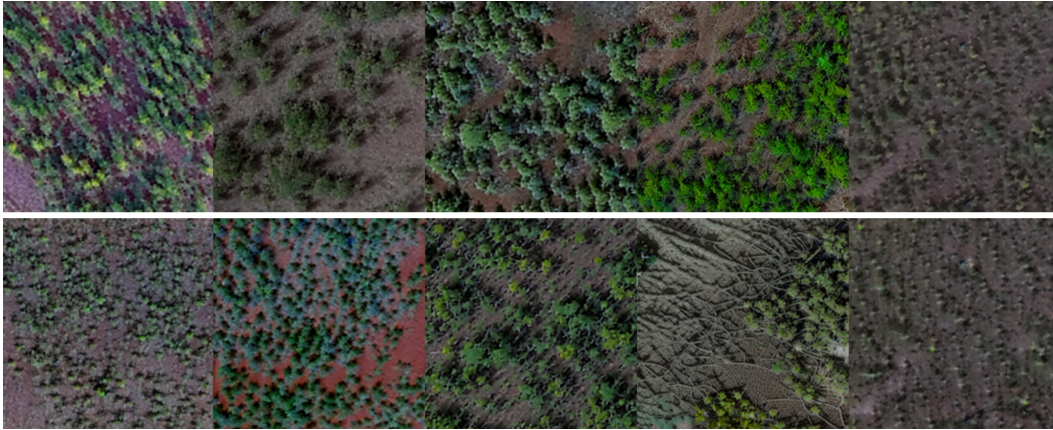


Figure 17: Here we show examples of synthetic images generated from the leafy spurge dataset with DA-Fusion methods. The top row shows output where images are pooled to fine-tune a single token per class. The bottom row shows examples where tokens are generated specifically for each image. Source images, inference hyperparameters, and seed are otherwise identical in each column.

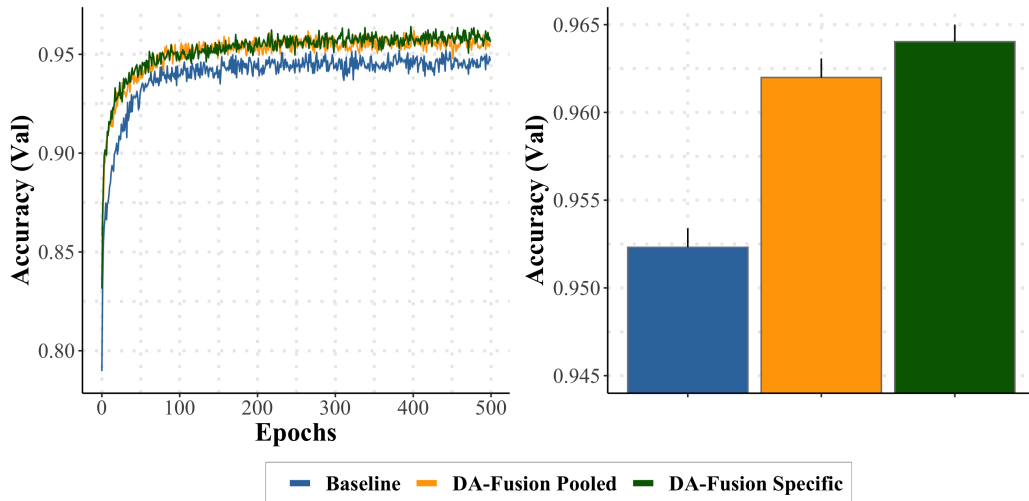


Figure 18: Cross-validated accuracy of leafy spurge classifiers when trained with baseline augmentations versus DA-Fusion methods on the full dataset. In addition to the benefits of DA-Fusion in few-shot contexts, we also find our method improves performance on larger datasets. Generating image-specific tokens (green line and bar) offers the most gains over baseline, though at the cost of greater compute.